Rare Metal Materials and Engineering
Volume 51, Issue 7, July 2022
Available online at www.rmme.ac.cn

Science Press

Cite this article as: Li Wei, Liu Lintao, Li Zhengxian, et al. Performance of Amorphous Carbon-Coated Titanium Bipolar Plate in PEMFC with Different Fluoride Ion Contents[J]. Rare Metal Materials and Engineering, 2022, 51(07): 2370-2378.

ARTICLE

Performance of Amorphous Carbon-Coated Titanium Bipolar Plate in PEMFC with Different Fluoride Ion Contents

Li Wei[1,3], Liu Lintao[2], Li Zhengxian[1,2], He Fei[2], Li Longbo[4], Lv Haibing[2]

[1] Xi'an University of Architecture and Technology, Xi'an 710055, China; [2] Northwest Institute for Nonferrous Metal Research, Xi'an 710016, China; [3] Sichuan University of Science & Engineering, Yibin 644002, China; [4] Northeastern University, Shenyang 110004, China

Abstract: The amorphous carbon coating was synthesized on the TA2 substrate surface by direct current balanced magnetron sputtering. The corrosion resistance and conductivity of TA2 substrate and amorphous carbon coating were analyzed by electrochemical and surface contact resistance tests in proton exchange membrane fuel cell (PEMFC) with different F^- contents. The results show that the corrosion resistance and conductivity of amorphous carbon-coated TA2 alloy are better than those of bare TA2 substrate. When the F^- content is increased from 1×10^{-6} mol/L to 1×10^{-3} mol/L, the defect density of TA2 substrate and amorphous carbon coating is increased, indicating the decreased corrosion resistance of both materials. The amorphous carbon coating at potential of 0.6 V demonstrates the corrosion current density of 0.68 μA/cm^2 in the F^- environment with high content (1×10^{-3} mol/L), still providing a good protection for TA2 substrate. Moreover, the amorphous carbon coating can also improve the surface conductivity of the TA2 substrate: the interface contact resistance decreases from 76.40 mΩ·cm^2 (TA2 substrate) to 6.52 mΩ·cm^2.

Key words: titanium bipolar plate; amorphous carbon coating; corrosion resistance; electrical conductivity

The hydrogen energy attracts extensive attention due to its wide source, high efficiency, and eco-friendly economy[1-3]. The proton exchange membrane fuel cells (PEMFCs) can directly convert the chemical energy of hydrogen into electricity and heat, and thus are widely used in transportation fields by the virtue of high efficiency, low temperature operation, and rapid start-up[4-6]. As the skeleton of PEMFC, the bipolar plate has multiple functions, such as reactive gas arrangement, current collection, and removal of reaction products. Besides, it has a key effect on the volume, quality, and power density of PEMFC stack[7-10]. Metal is the mainstream material of PEMFC bipolar plate on account of the controllable thin thickness (0.1~1 mm), developed processing techniques, and good electrical and thermal conductivities[11]. Compared with the stainless steels, titanium alloys not only exhibit excellent corrosion resistance, but also have low density, which can improve the quality power density and service stability of PEMFC stack[12,13]. The excellent corrosion resistance of the titanium bipolar plate mainly originates from its dense passivation film in the air and PEMFC. However, the resistivity of passivation film is high, significantly increasing the interface contact resistance (ICR) between the bipolar plate and the gas diffusion layer (GDL). Therefore, the electrical energy is dissipated as waste heat, weakening the cell performance[14-17]. Thus, it is necessary to modify the surface of the titanium bipolar plate to further improve its surface conductivity and corrosion resistance.

During the operation of the hydrogen fuel vehicle, the proton exchange membrane releases F^- into PEMFC environment due to the local chemical and thermal degradations. In addition, the metal cations (Fe, Cr, and Ni ions) produced by the corrosion of the bipolar plate can promote the generation of hydroxyl radicals, which further accelerates the chemical attenuation of the proton exchange membrane. The content of F^- ions in cathode and anode environment is much higher than that of other ions (H^+, SO_4^{2-}) after long-term operation of PEMFC stack[18]. Moreover, the F^- produced by the degradation of the proton exchange

---

Received date: July 14, 2021
Foundation item: Shaanxi Provincial Natural Science Basic Research Program (2019JQ-940, 2019JM-619); Panzhihua Science and Technology Department Project (2020CY-G-5)

Corresponding author: Li Zhengxian, Ph. D., Professor, Northwest Institute for Nonferrous Metal Research, Xi'an 710016, P. R. China, Tel: 0086-29-86231077, E-mail: lzxqy725@163.com

membrane may change the corrosion behavior of the bipolar plate[19]. At present, the F^- ion content in the simulated PEMFC solution is usually 2×10^{-6}~5×10^{-6} mol/L, which is much lower than the F^- content in the long-term service environment (10^{-5}~10^{-4} mol/L)[20,21].

Therefore, in this research, the direct current (DC)-balanced magnetron sputtering was used to prepare an amorphous carbon coating on TA2 substrate. The corrosion behavior was evaluated through the potentiodynamic polarization tests, electrochemical impedance spectrum (EIS) tests, and Mott-Schottky (M-S) tests to reveal the corrosion mechanism of TA2 substrate and TA2 with amorphous carbon coatings in PEMFC environment with different F^- contents (1×10^{-6}, 1×10^{-5}, 1×10^{-4}, and 1×10^{-3} mol/L).

1 Experiment

The single crystal (100) silicon and TA2 substrate with a size of 100 mm×50 mm×0.1 mm were used to deposit the coatings. The TA2 substrate was ultrasonically cleaned by metal cleaning agent, ethanol, and deionization water, and then dried in an oven. The amorphous carbon coatings were deposited by DC-balanced magnetron sputtering equipment, and the sputtering targets were graphite and titanium targets with the purity of 99.99%. When the vacuum degree is below 3×10^{-3} Pa, the Ar gas was introduced to increase the vacuum degree to 1.0 Pa, and then the bias voltage was adjusted to −1000 V to pre-clean the substrate by Ar^+ plasma for 20 min. The Ti buffer layer was firstly deposited with a titanium target current of 3 A for 30 min. Then the titanium target current gradually decreased to 0 A and the graphite target current increased to 3 A to deposit the amorphous carbon coating for 2 h. The temperature was kept at 300 °C during the deposition process.

The surface and cross-section morphologies of the amorphous carbon coating were observed by field emission scanning electron microscope (SEM, JSM6700F, JEOL, Japan), and the energy dispersive spectrometer (EDS) was used to analyze the surface element composition of the coatings. The Raman spectrometer (InVia Qontor, Renishaw, England) with a laser wavelength of 532 nm was used to examine the phase composition of amorphous carbon coating. The phase composition was further characterized by X-ray photoelectron spectroscopy (XPS, ESCALAB 250Xi, Thermo Fisher Scientific, USA).

The corrosion tests were performed by electrochemical workstation (Zahner-Zennium) with a three-electrode electrochemical system, where a saturated calomel electrode (SCE), platinum sheet, and the specimen were served as reference electrode, counter electrode, and working electrode, respectively. The testing area of specimen was 1 cm^2, and the other parts were sealed with 706 silica gel. In order to simulate the working environment of PEMFC, H_2SO_4 with pH =3 was used as the solution containing different contents of F^- (1×10^{-6}, 1×10^{-5}, 1×10^{-4}, and 1×10^{-3} mol/L), and the test temperature was 70 °C. The sweep rate of the potentiodynamic polarization test was 1 mV/s. The EIS test was conducted at open current potential (OCP) with the frequency of 10^{-2}~10^{5} Hz, and the excitation voltage was 10 mV. M-S test was conducted with the potential of 0~1 V, and the data acquisition frequency was 100 Hz.

The porous carbon paper (YLS-35, TORAY, Japan) was selected to simulate GDL in PEMFC. The specimen was placed between two carbon papers, and then they were placed between two copper plates[21]. Through the universal testing machine, the pressure between the bipolar plate and GDL was controlled, and then DC low resistance tester (TH2516B, Tonghui, China) was used to measure ICR of the specimens.

2 Results and Discussion

2.1 Composition and microstructural characterization

Fig. 1a exhibits the surface microstructure of TA2 substrate. The striped rolling lines can be observed on the TA2 substrate surface, and there is no obvious change after the deposition of amorphous carbon coating (Fig. 1b). Fig. 1c shows the microstructure of the amorphous carbon coating, which is composed of granular structures with a size of 50~70 nm, and the coating surface is flat and dense without obvious defects. The cross-section morphology of the amorphous carbon coating shows a columnar crystal structure, which is composed of Ti intermediate layer with a thickness of about 100 nm and an amorphous carbon layer with a thickness of 726 nm (Fig. 1d). The coating is tightly bonded with substrate without obvious pinholes or micro-cracks.

The surface elements of TA2 substrate and amorphous carbon coating were analyzed by EDS, and the results are shown in Fig. 2. The TA2 substrate only contains Ti (Fig. 2a), and the amorphous carbon coating mainly contains Ti and C (Fig. 2b). Since the detection depth of EDS analysis is greater than 1 μm and the thickness of the amorphous carbon coating is only 726 nm, the element distributions in Ti intermediate layer and TA2 substrate can all be detected.

The Raman spectroscopy was used to further characterize the carbon structure of coating, and the result is shown in Fig. 3b. A typical asymmetric structure of amorphous carbon can be observed, mainly consisting of D peak and G peak. The G peak corresponds to the in-plane vibration of the sp^2 carbon in the form of ring or chain, while the D peak indicates the A_{1g} band at the edge of the graphite[22]. Gaussian function is used to fit the Raman peak, and the integrated area intensity ratio of peak D to peak G (I_D/I_G) is 2.91. Thus, the position of G peak is 1574 cm^{-1}, indicating that there are more sp^2 hybrid structures in the amorphous carbon coating[23]. The high content of sp^2 structures in the coating is conducive to the electrical properties of coating.

The Raman spectroscopy can only perform qualitative detection on the bonding status of amorphous carbon coatings. Therefore, it is necessary to quantitatively analyze the sp^2 and sp^3 hybridization ratios of coatings by XPS. The amorphous carbon usually has sp^2 and sp^3 structures, and the coating can adsorb oxygen atoms from the outside through the preparation process. Therefore, the peak fitting analysis of the C 1s peak

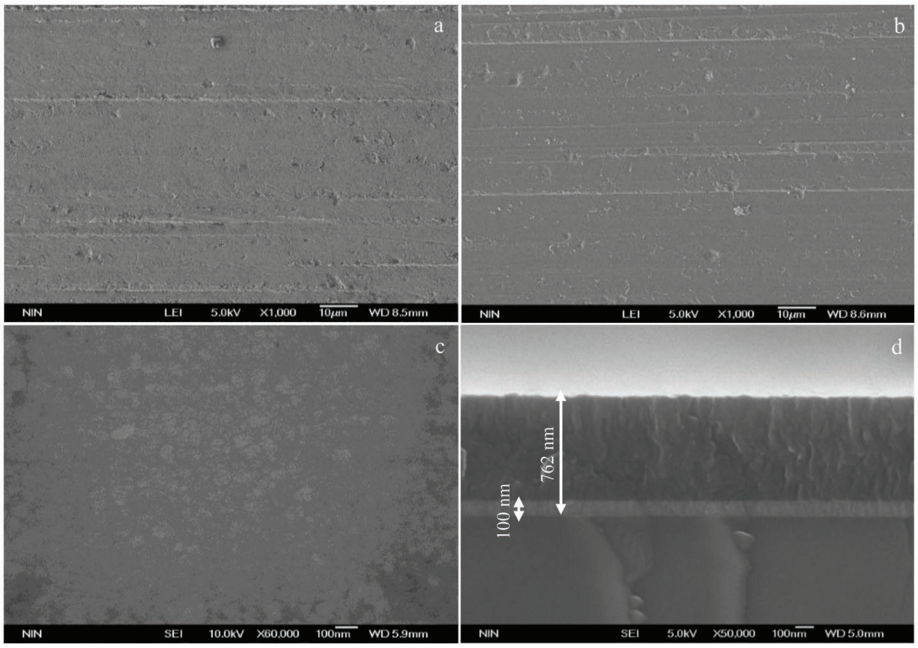

Fig.1 Surface morphologies of TA2 substrate (a) and amorphous carbon coating (b, c); cross-section morphology of amorphous carbon coating (d)

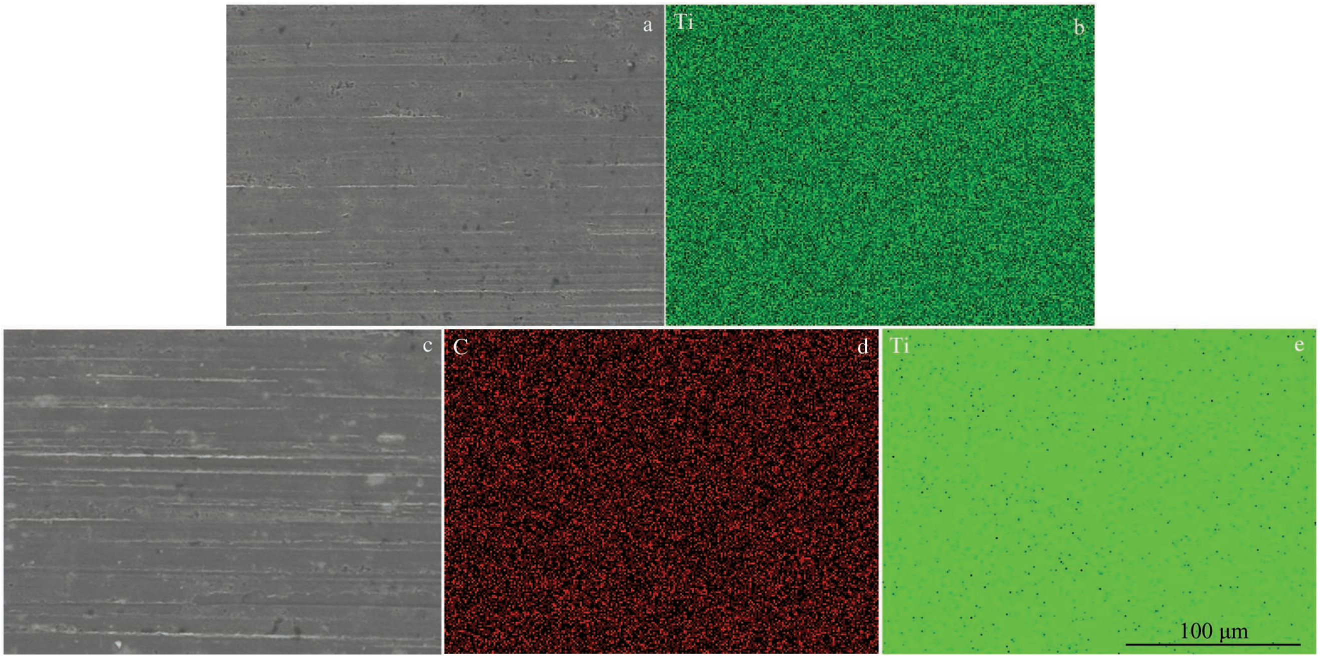

Fig.2 SEM images (a, c) and EDS element distributions of Ti (b, e), C (d) in TA2 substrate (a, b) and amorphous carbon coating (c~e)

was conducted, and the fitting function is Lorentz-Gauss (20% Lorentz). The C 1s peak is fitted by four small peaks, namely, sp^2 (284.7 eV), sp^3 (285.6 eV), C-O (286.9 eV), and C=O (286.9 eV). The results are shown in Fig. 3d. It can be seen that the sp^2 hybrid content in the amorphous carbon is 56.06% according to the peak area ratio, which is consistent with the results of Raman analysis. In addition, it can be seen from Fig. 3a and 3c that the TA2 substrate surface is mainly composed of Ti element and a small amount of O due to the surface oxidation of TA2 substrate.

2.2 Corrosion behavior

2.2.1 Potentiodynamic polarization

Fig. 4a shows the potentiodynamic polarization curves of bare TA2 substrate in PEMFC solutions with different F^- contents. The corrosion potential (E_{corr}) and corrosion current density (i_{corr}) were calculated by the Tafel extrapolation method, as listed in Table 1. With increasing the F^- content in the solution, E_{corr} of the bare TA2 substrate is gradually

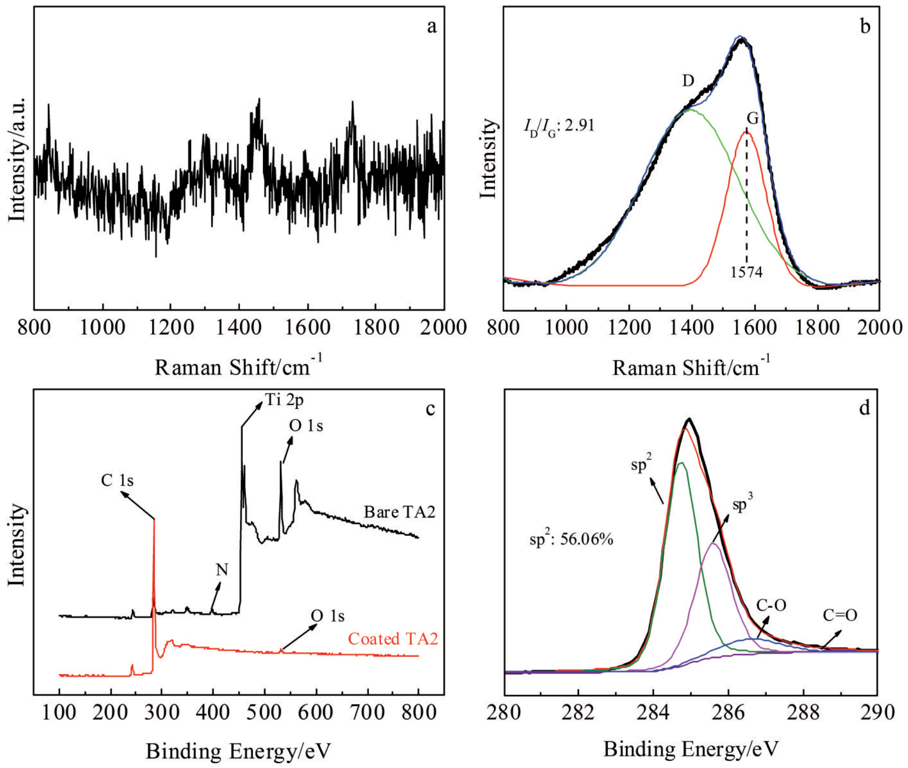

Fig.3 Raman spectra of TA2 substrate (a) and amorphous carbon coating (b); XPS spectra of bare and coated TA2 substrates (c); high-resolution spectra of C 1s in amorphous carbon coating (d)

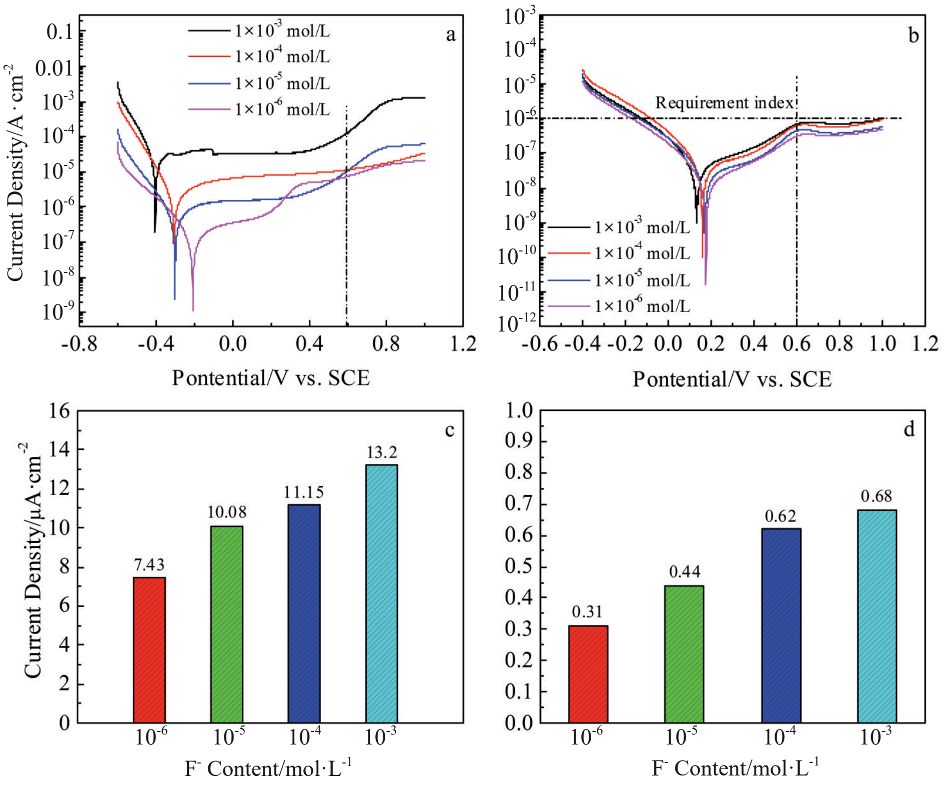

Fig.4 Potentiodynamic polarization curves of bare (a) and coated (b) TA2 substrates in solution with different F^- contents; corrosion current densities of bare (c) and coated (b) TA2 substrates at cathode potential of 0.6 V

decreased from −0.213 V to −0.405 V, and i_{corr} is also increased from 1.11×10^{-7} A·cm^{-2} to 2.05×10^{-5} A·cm^{-2}. The corrosion behavior of bipolar plates in PEMFC environment is different from that at free corrosion potential, so the

Table 1 Electrochemical parameters of bare and coated TA2 substrates

Specimen	F^- content/mol·L^{-1}	E_{corr}/V	i_{corr}/A·cm^{-2}
Bare	10^{-6}	−0.213	1.11×10^{-7}
	10^{-5}	−0.304	5.02×10^{-7}
	10^{-4}	−0.307	1.79×10^{-6}
	10^{-3}	−0.405	2.05×10^{-5}
Coated	10^{-6}	0.182	1.19×10^{-8}
	10^{-5}	0.175	2.11×10^{-8}
	10^{-4}	0.162	3.28×10^{-8}
	10^{-3}	0.133	3.67×10^{-8}

instantaneous corrosion current density of the bare TA2 substrate at a cathode potential of 0.6 V was further investigated, as shown in Fig. 4c. The corrosion current density is 7.43 μA/cm^2 in the solution with 1×10^{-6} mol/L F^- ions. With further increasing the F^- content to 1×10^{-3} mol/L, the corrosion current density is continuously increased to 13.20 μA/cm^2. This result shows that the protective effect of the passive coating on TA2 substrate continues to decrease with increasing the F^- content.

With the deposited coating, E_{corr} is greatly improved by approximately 500 mV, compared with that of the bare TA2 substrate (Fig. 4b). E_{corr} of all the coated TA2 substrates is about 0.2 V, which is greater than the anode potential (−0.1 V) of PEMFC, thereby providing a good cathodic protection for the bipolar plate in PEMFC environment. The i_{corr} of the coated TA2 substrate is also increased with increasing the F^- content, but the increment is small, indicating that the amorphous coating is less sensitive to the variation of F^- content. At the cathode potential of 0.6 V, with increasing the F^- content, the corrosion current density is gradually increased from 0.31 μA/cm^2 to 0.68 μA/cm^2 (Fig.4d). It is worth noting that the corrosion current density of the coated TA2 substrate is 0.68 μA/cm^2 under the condition of high F^- content (1×10^{-3} mol/L), which still meets the requirement index. This result shows that the amorphous carbon coating can effectively prevent the entry of F^- ions and form a good protection for the TA2 substrate.

2.2.2 Mott-Schottky analysis

The passivation film on the metal surface is considered as a corrosion product layer with high defect density, which usually reflects the semiconductor characteristics[24]. The donor density, acceptor density, and flat band potential of the passivation film can be obtained by M-S curves. The formation mechanism of the passive film can also be obtained, and the corrosion resistance of the passivation film in different solutions was analyzed. The metal passivation film is usually divided into the N-type and P-type semiconductors, which can be expressed as follows:

$$\frac{1}{C^2}=\frac{2}{\varepsilon_0\varepsilon eN_D}\left(E-E_{fb}-\frac{KT}{e}\right)\text{ for N-type semiconductor} \quad (1)$$

$$\frac{1}{C^2}=-\frac{2}{\varepsilon_0\varepsilon eN_A}\left(E-E_{fb}-\frac{KT}{e}\right)\text{ for P-type semiconductor} \quad (2)$$

where C is the space charge capacitance (F·cm^{-2}); N_D and N_A are the donor density and acceptor density (cm^{-3}), respectively; ε represents the dielectric constant for Ti oxide (56 F·cm^{-1})[25,26]; ε_0 is the permittivity of vacuum (8.854×10^{-14} F·cm^{-1}); E is the potential; E_{fb} is the flat band potential; K is the Bolsman constant; T is the absolute temperature.

Fig. 5 shows M-S curves of bare TA2 substrate in solution with different F^- contents. The slope of the M-S curves is all positive of 0~1.4 V, which indicates that the passivation film on TA2 substrate is an N-type semiconductor. The M-S curve of passivation film can be basically divided into two linear regions (MN and PQ), and their slopes are different, indicating that the contents of two donors in the passivation film are different. When the F^- content increases, the capacitance of the passivation film continues to increase under the same scanning voltage. The increase in the capacitance of the passivation film indicates that more corrosive liquid is penetrated into the passivation film and the substrate, and thus the defects of the passivation film are increased. In addition, the slope value of the linear region of M-S curves is continuously decreased with increasing the F^- content, indicating that the number of point defects in the passivation film is increased. This reveals that F^- reduces the protective effect of the passivation film on the TA2 substrate.

A linear relationship between capacitance C^{-2} and potential E (0.4~1.0 V) is obtained, and the results are listed in Table 2. The slope (K) of the PQ region is gradually decreased from 4.72 to 2.70 with increasing the F^- content. The relationship between K and donor density of passivation film (N_D) can be expressed by Eq.(3), as follows:

$$N_D=\frac{2}{\varepsilon_0\varepsilon eK} \quad (3)$$

When the F^- content is 1×10^{-6} mol/L, the defect density of the passivation film is 5.33×10^{19} cm^{-3}. However, the defects of the passivation film increases to 9.32×10^{19} cm^{-3} when the F^- content is 1×10^{-3} mol/L. According to the point defect model (PDM), the higher the defect density in the passivation film, the lower the corrosion resistance[27]. The corrosive F ions are mainly adsorbed onto the oxygen vacancies of the passive film and can induce the M-S pair reaction, therefore

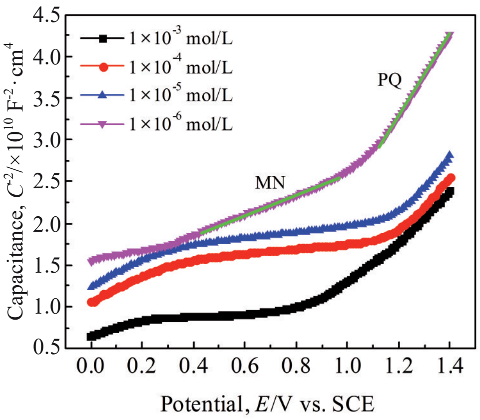

Fig.5 M-S curves of bare TA2 substrates in solution with different F^- contents

Table 2 Donor densities and flat band potentials of passive films on TA2 substrate

F^- content/mol·L^{-1}	$K/\times10^{10}$	N_D or $N_A/\times10^{19}$ cm^{-3}	E_{fb}/V
10^{-3}	2.70	9.32	0.810
10^{-4}	3.19	7.89	0.798
10^{-5}	3.49	7.21	0.712
10^{-6}	4.72	5.33	0.632

generating more cation vacancy/oxygen vacancy pairs. The generated oxygen vacancies continue to react with F^-, resulting in more cation vacancies and hindering the growth of the passivation film. Therefore, the dissolution rate of the passivation film is greater than its generation rate, causing the occurrence and expansion of pitting corrosion and increasing the defect density of the passivation film. Moreover, F^- can also react with the protective oxide film on substrate to form the soluble titanium-fluoride compounds, which results in the solution of the passivation film on TA2 substrate and increases the porosity[28], as follows:

$$TiO_2 + 4H^+_{aq} + 6F^-_{aq} \rightarrow Ti_2F_6^{2-} + 2H_2O \quad (4)$$

The value of the flat band potential (E_{fb}) can be obtained by the intersection of the straight line and the x-axis, and its value is shown in Table 2. The E_{fb} of the passivation film of TA2 substrate is gradually decreased with increasing the F^- content. The Nestain expression of E_{fb} can be expressed by Eq. (5)[29], as follows:

$$E_{fb} = \frac{E_0^f}{e} + \Delta\varphi_H \quad (5)$$

where E_0^f is the potential drop of the space charge layer, and $\Delta\varphi_H$ is the potential difference between the electrode surface and the outer Helmholz. Since E_0^f is zero at the flat band potential, $\Delta\varphi_H$ is determined by the size of E_{fb}. The smaller the E_{fb} value, the better the corrosion resistance of passivation film. Therefore, the passivation film has a better protective ability to TA2 substrate at lower F^- content.

Fig. 6 shows the M-S curves of amorphous carbon coating in PEMFC solution with different F^- contents. The amorphous carbon coating mainly shows the N-type semiconductor behavior in the scanning range of 0~1.4 V. The slope of the M-S curves is decreased with increasing the F^- content, indicating that F^- can also be adsorbed on the surface of the amorphous carbon coating, which promotes the defects in coating. The capacitance of the amorphous carbon coating is smaller than that of bare TA2 substrate at the same F^- content, indicating that the coating has better corrosion resistance compared with the TA2 passivation film. The amorphous carbon has high conductivity (close to graphite), so its vacuum dielectric constant is much greater than that of TiO_2 (56 F/cm). Therefore, the defect density of the amorphous carbon coating is much lower than that of the passivation film, resulting in good protection for TA2 substrate.

2.2.3 EIS analysis

The EIS test results of bare and coated TA2 substrates in simulated PEMFC environment with different F^- contents after the steady state of OCP are shown in Fig. 7. With increasing the F^- content, the arc radius of capacitance of bare TA2 substrate is continuously decreased, suggesting that F^- can reduce the charge transfer resistance between the solution and the substrate, and resulting in the decrease in corrosion resistance of bare TA2 substrate (Fig. 7a). It can be found from Fig. 7b and 7c that the resistance and phase angle of bare TA2 substrate in the middle and low frequency regions continue to decrease with increasing the F^- content, which further indicates that F^- reduces the protective effect of the passivation film on the TA2.

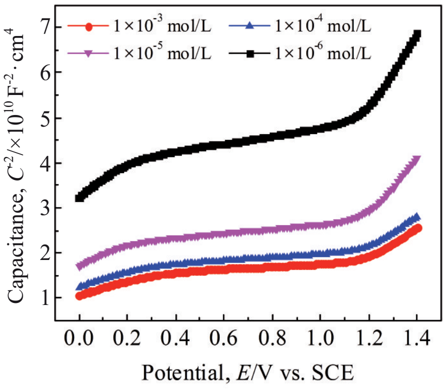

Fig.6 M-S curves of coated TA2 substrates in solution with different F^- contents

The Nyquist plots of amorphous carbon coated TA2 substrate at different F^- contents also show a single semicircle (Fig. 7d). It can be seen that amorphous carbon coated TA2 substrates have obviously bigger radius than the bare TA2 substrate does, indicating better corrosion resistance. The arc radius of capacitance of coated substrate is decreased with increasing the F^- content, indicating that F^- also reduces the corrosion resistance of the amorphous carbon coating. The impedance value of the coating continuously increases to 10^6 in the low frequency region, which is higher than that of bare TA2 substrate (10^4~10^5). In addition, with increasing the F^- content, the phase angle in the low frequency region is gradually decreased from 73° to 58° (Fig. 7f), but it is still much higher than that of the bare TA2 substrate (28°). This indicates that the amorphous carbon coating has better corrosion resistance at the same F^- content.

In order to further analyze the electrochemical impedance of the TA substrates, the equivalent circuit diagrams with a one-time constant (Fig. 7a) and a two-time constant (Fig. 7d) are used to analyze the bare and coated TA2 substrates[30], respectively. The fitting results are listed in Table 3. R_s is the solution resistance between the working electrode and the reference electrode; R_c is the coating resistance; Q_c is the non-ideal capacitance of the coating; R_{ct} is the charge transfer resistance; Q_{ct} is the non-ideal double layer capacitance of charge transfer between substrate and liquid; N_c and N_{ct} are coefficients of coating and double layer, respectively. With increasing the F^- content, the R_{ct} of bare TA2 substrate is gradually decreased from 1.59×10^5 Ω·cm^2 to 2.15×10^4 Ω·cm^2,

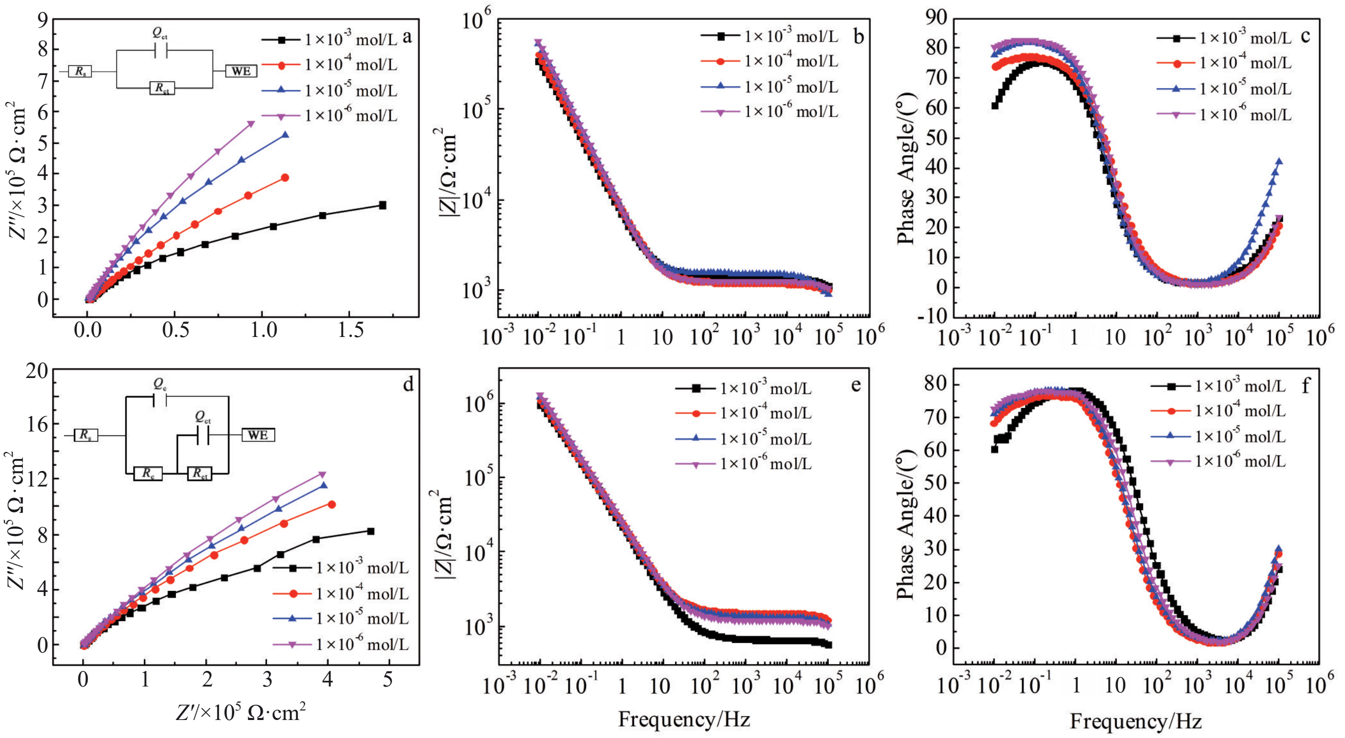

Fig.7 Nyquist plots (a, d) and Bode plots (b, c, e, f) of bare (a~c) and coated (d~f) TA2 substrates in solution with different F^- contents: relationships of resistance (b, c) and phase angle (e, f) with frequency

Table 3 EIS fitting results of bare and coated TA2 substrates

Specimen	F^- content/mol·L^{-1}	R_s/Ω·cm^2	Q_c/μF·cm^{-2}	N_c	R_c/×10^3 Ω·cm^2	Q_{ct}/μF·cm^{-2}	N_{ct}	R_{ct}/Ω·cm^2	R_p/Ω·cm^2
Bare	10^{-3}	1.97	-	-	-	102.1	0.943	2.15×10^4	-
	10^{-4}	1.86	-	-	-	129.5	0.948	2.63×10^4	-
	10^{-5}	1.54	-	-	-	102.1	0.943	3.50×10^4	-
	10^{-6}	1.44	-	-	-	36.7	0.914	1.59×10^5	-
Coated	10^{-3}	2.46	3.55×10^2	0.683	1.08	8.41	0.876	-	1.97×10^6
	10^{-4}	1.22	1.40×10^3	0.953	1.38	9.28	0.865	-	6.42×10^6
	10^{-5}	4.09	2.62×10^3	0.905	1.36	8.82	0.875	-	8.72×10^6
	10^{-6}	5.69	1.51×10^3	0.944	1.13	8.26	0.872	-	1.24×10^7

and the polarization resistance ($R_p=R_c+R_{ct}$) of the coating is gradually decreased from 1.24×10^7 Ω·cm^2 to 1.97×10^6 Ω·cm^2. The higher the R_p value, the larger the charge transfer resistance between the corrosion solution and the TA2 substrate. This shows that F^- can reduce the R_{ct} of bare and coated TA2 substrates and increase the charge transfer between TA2 substrate and the solution, therefore reducing the corrosion resistance of TA2 substrates. However, the polarization resistance of amorphous carbon coating is much higher than that of bare TA2 substrate at the same F^- content, which can effectively block the entry of corrosion ions and form a good protection for the substrate.

2.3 ICR analysis

ICR originates from the interface between bipolar plate and GDL and has a key influence on the output power of the PEMFC[30]. Fig. 8 displays the relationship between ICR and the pressure. It is clear that ICR of bare and coated TA2 substrates decreases sharply at first, and quickly becomes stable at high pressure (1.0 MPa). In addition, ICR of bare

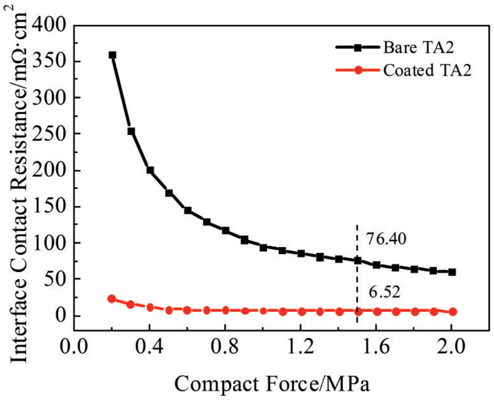

Fig.8 Interface contact resistance of bare and coated TA2 substrates

TA2 substrate is always higher than that of the coated one under the same pressure. ICR is affected by the surface composition under the same pressure. The resistivity of the passivation film on the TA2 substrate surface is high, which increases ICR of bare TA2 substrate. The oxide on the TA2 substrate surface is reduced by glow cleaning before deposition, and the amorphous carbon coating has a high sp^2 content, which can increase the electron transfer between the coating and GDL, thereby greatly reducing ICR value. Under the PEMFC standard assembly pressure of 1.5 MPa, ICR value of the amorphous carbon coating is only 6.52 $m\Omega\cdot cm^2$, which is much smaller than that of bare TA2 substrate (76.40 $m\Omega\cdot cm^2$) and can meet the common requirements (<10 $m\Omega\cdot cm^2$).

3 Conclusions

1) The amorphous carbon coating is prepared on the TA2 surface by direct current-balanced magnetron sputtering, which greatly improves the surface conductivity of TA2 substrate, and the interface contact resistance is reduced from 76.40 $m\Omega\cdot cm^2$ (bare TA2) to 6.52 $m\Omega\cdot cm^2$ (coated TA2) under pressure of 1.5 MPa.

2) The F^- content in the proton exchange membrane fuel cell solution has an important influence on the corrosion resistance of TA2 substrate. F^- can be adsorbed and penetrated to the passivation film, therefore not only hindering the formation of a new passivation film, but also accelerating the dissolution of the passivation film. As a result, the corrosion current density of TA2 substrate at 0.6 V is increased from 7.43 $\mu A/cm^2$ to 13.20 $\mu A/cm^2$ with increasing the F^- content from 1×10^{-6} mol/L to 1×10^{-3} mol/L. The corrosion current density of coated TA2 substrate is greatly reduced to 0.68 $\mu A/cm^2$ even at a high F^- content (1×10^{-3} mol/L), which still meets the requirement.

3) The passivation film of TA2 substrate exhibits the characteristics of N-type semiconductor. With increasing the F^- content, the defect density is gradually increased from 5.33×10^{19} cm^{-3} to 9.32×10^{19} cm^{-3}. F^- ions can increase the defects in amorphous carbon coating, but the overall defect density of coated TA2 substrate is much lower than that of the bare TA2 substrate.

References

1 Zhao Y Q, Mao Y J, Zhang W X *et al. International Journal of Hydrogen Energy*[J], 2020, 45(43): 23 174

2 Chen H C, Xu S C, Pei P C *et al. International Journal of Hydrogen Energy*[J], 2019, 44(11): 5437

3 Qian Yang, Xu Jiang. *Rare Metal Materials and Engineering*[J], 2017, 46(4): 1033 (in Chinese)

4 Liu Jiawei, Li Qi, Chen Weirong *et al. IEEE Transactions on Transportation Electrification*[J], 2019, 5(1): 271

5 Li Q, Wang T H, Dai C H *et al. IEEE Transactions on Vehicular Technology*[J], 2018, 67(7): 5658

6 He K, Zhang C, He Q B *et al. International Journal of Hydrogen Energy*[J], 2020, 45(56): 32 355

7 Jin J, Liu H J, Zheng D C *et al. International Journal of Hydrogen Energy*[J], 2018, 43(21): 10 048

8 Yang L J, Yu H J, Jiang L J *et al. Journal of Power Sources*[J], 2010, 195(9): 2810

9 Jin J, He Z, Zhao X H. *Materials Chemistry and Physics*[J], 2020, 245: 122 739

10 Yi P Y, Li X B, Yao L *et al. Energy Conversion & Management*[J], 2019, 183: 65

11 Makkus R C, Janssen A H H, De Bruijn F A *et al. Fuel Cells Bulletin*[J], 2000, 3(17): 5

12 Lu J L, Liang T X, Guo W L. *International Journal of Hydrogen Energy*[J], 2015, 40(33): 10 382

13 Zhang P C, Hao C M, Han Y T *et al. Surface and Coatings Technology*[J], 2020, 397: 126 064

14 Shi Jiefu, Zhang Pengchao, Han Yuetong *et al. International Journal of Hydrogen Energy*[J], 2020, 45(16): 10 050

15 Gao P P, Xie Z Y, Wu X B *et al. International Journal of Hydrogen Energy*[J], 2018, 43(45): 20 947

16 Jin J, He Z, Zhao X H. *International Journal of Hydrogen Energy*[J], 2020, 45(22): 12 489

17 Xu J, Huang H J, Li Z Y *et al. Journal of Alloys and Compounds*[J], 2016, 663: 718

18 Agneaux A, Plouzennec M H, Antoni L *et al. Fuel Cells*[J], 2006, 6(1): 47

19 Liu X D, Funakubo H, Noda S *et al. Journal of the Electrochemical Society*[J], 2001, 148(3): 227

20 Yang Y, Guo L J, Liu H. *Journal of Power Sources*[J], 2010, 195(17): 5651

21 Yang Y, Guo L J, Liu H T. *International Journal of Hydrogen Energy*[J], 2012, 37(18): 13 822

22 Bi F F, Peng L F, Yi P Y *et al. Journal of Power Sources*[J], 2016, 314: 58

23 Tay B K, Shi X, Tan H S *et al. Surface and Coatings Technology*[J], 1998, 105(1-2): 155

24 Simões A M P, Ferreira M, Rondot B *et al. Journal of the Electrochemical Society*[J], 1990, 137(1): 82

25 Marsh J, Gorse D. *Electrochimica Acta*[J], 1998, 43(7): 659

26 Ju P F, Zuo Y, Tang Y M *et al. Corrosion Science*[J], 2013, 66: 330

27 Harrington S P, Wang F, Devine T M. *Electrochimica Acta*[J], 2010, 55(13): 4092

28 Wang Z B, Hu H X, Liu C B *et al. Electrochimica Acta*[J], 2014, 135: 526

29 Yang Y, Ning X H, Tang H S *et al. Applied Surface Science*[J], 2014, 320: 274

30 Ghorbani M M, Taherian R, Bozorg M. *Materials Chemistry and Physics*[J], 2019, 238: 121 916

钛双极板无定型碳涂层在PEMFC不同氟离子环境中的性能

李　伟[1,3]，刘林涛[2]，李争显[1,2]，何　飞[2]，李龙博[4]，吕海兵[2]
(1. 西安建筑科技大学，陕西 西安 710055)
(2. 西北有色金属研究院，陕西 西安 710016)
(3. 四川轻化工大学，四川 宜宾 644002)
(4. 东北大学，辽宁 沈阳 110004)

摘　要：采用直流平衡磁控溅射在TA2基材表面制备了无定型碳涂层，并采用电化学和表面接触电阻测试分析了TA2基材和无定型碳涂层在质子交换膜燃料电池（PEMFC）不同F^-浓度环境中的耐腐蚀性和导电性。无定型碳涂层的耐腐蚀性和导电性均优于TA2基材，随着F^-浓度由1×10^{-6} mol/L逐渐增加到1×10^{-3} mol/L，TA2基材和无定型涂层的缺陷密度增加，试样耐腐蚀性均有所下降。在高F^-浓度环境中（1×10^{-3} mol/L），无定型碳涂层在0.6 V电位下的腐蚀电流密度为0.68 $\mu\mathrm{A/cm^2}$，依然能够对基材形成良好的保护。此外，TA2基材表面制备无定型碳涂层后，试样的表面导电性有所提升，其界面接触电阻值由76.40 $\mathrm{m\Omega\cdot cm^2}$（TA2）下降至6.52 $\mathrm{m\Omega\cdot cm^2}$。

关键词：钛双极板；无定型碳涂层；耐腐蚀性；导电性

作者简介：李　伟，男，1989年生，博士，四川轻化工大学，四川 宜宾 644002，E-mail：liweibuqi@163.com